

# SYMBOLIC DYNAMICS OF THE COLLINEAR THREE-BODY PROBLEM

SAMUEL R. KAPLAN

**ABSTRACT.** Solutions to the collinear three-body problem which do not end in triple collision pass through an infinite number of binary collisions. Given three masses, we show that four geometric quantities generate a finite description of itineraries of binary collisions. In the best circumstances, this description is semi-conjugate to a Poincaré map of the flow. For other cases these quantities give upper and lower bounds on the itineraries which can occur. In addition to describing the dynamics of the collinear three-body problem, the results of this paper rederives the existence of oscillatory motion in the  $N$ -body problem for  $N \geq 3$ .

## 1. INTRODUCTION

In the seventeenth century, Newton formulated the universal law of gravitation and completely solved the two-body problem. Moreover, his methods confirmed Kepler's laws of planetary motion. After this grand success Newton turned his fluxions to the motions of the Earth, moon and sun. He eventually gave up working on this three-body problem, saying it gave him headaches [10].

In the intervening years much work was done on the three-body problem generating new techniques and new questions. After Poincaré showed that chaotic behavior can occur in the restricted three-body problem [13], the search for a complete solution halted abruptly. Poincaré's result changed the issue from trying to solve an initial value problem to asking what behaviors can occur in the three-body problem.

A critical step in understanding what dynamics can occur in the three-body problem was identifying behavior near triple-collision. McGehee made a great leap forward in this field in 1974 with his analysis of triple-collision behavior in the collinear three-body problem [9]. He introduced a change of variable to what is now known as McGehee coordinates, in which the differential equations for Newton's universal law of gravitation are extended to triple collision. By understanding the dynamics at triple collision, one understands the dynamics near triple collision via continuity of the flow.

Generating a global analysis of the collinear three-body problem requires an understanding of how near-triple collision behavior effects the entire flow. Using ideas of Saari and Xia [14], Meyer and Wang undertook this endeavor [11], giving a nice picture of the geometry of the phase space for the collinear three-body problem.

Meyer and Wang's method of analysis involves generating a Poincaré slice to the flow and partitioning that slice with pieces of stable manifold for triple collision. Then in at least some part of the flow the regions generate a subshift of finite type on an infinite set of symbols. This is enough to show that chaotic behavior occurs in the collinear three-body problem. However, this result raises the question of

determining exactly what itineraries of binary collisions are allowed and how the set of allowed itineraries changes as the masses vary.

In order to gain insight on the role of geometry in the collinear three-body problem, the author chose to use McGehee coordinates. In contrast, Meyer and Wang choose coordinates so that binary collision is represented by a sink. Their approach has some advantages; however, in McGehee coordinates binary collisions are represented by half-planes. Thus, McGehee coordinates reveal more detail on how the stable manifold for triple collision intersects the Poincaré slice.

The crucial construction in this paper is the partition of a Poincaré slice into a finite number of regions bounded by pieces of stable manifold for triple collision. The Theorems in Section 5 give conditions on when this partition is Markov. When the partition is Markov, we can construct a semi-conjugacy from the Poincaré map to a directed graph and exactly describe the set of allowed itineraries. When the partition is not Markov, we can construct two sub-shifts of finite type, one containing all allowed sequences and one containing guaranteed sequences. These two sub-shifts serve as upper and lower bounds on the set of allowed itineraries.

For details of this approach applied to a model problem in which more detail can be explicitly computed, see [4, 5, 6, 7] which consider the dynamics of the collinear one-bumper two-body problem.

Except for very special cases, the conditions required by the theorems below can only be computed numerically. Even so, the theorems in this paper give a picture of what symbolic dynamics occur in the collinear three-body problem and what geometric quantities one needs to compute in order to describe those dynamics.

The symbolic dynamics of the collinear three-body problem are enough to guarantee the existence of special solutions (oscillatory motion) in the  $N$ -body problem (see the Corollary in Section 6).

## 2. HAMILTONIAN COORDINATES

We begin by stating the collinear three-body problem in Hamiltonian coordinates and then look at the regularized system in McGehee coordinates.

Three point masses have masses  $m_i > 0$  and positions  $q_1 \leq q_2 \leq q_3 \in \mathbb{R}$ . The potential energy is given by

$$(1) \quad U = \sum_{i>j} \frac{m_i m_j}{q_i - q_j}.$$

The motion of the particles under gravitational force is described by the systems of differential equations

$$(2) \quad m_i \ddot{q}_i = \nabla_{q_i} U, \quad i = 1, 2, 3$$

where  $\nabla_{q_i} U$  is the gradient of  $U$  with respect to  $q_i$ .

A position,  $(q_1, q_2, q_3)$  is called a *binary collision* if either  $q_1 = q_2$  or  $q_2 = q_3$ . If  $q_1 = q_2 = q_3$  the position is called a *triple collision*. The above system is defined everywhere except at binary and triple collisions. Given an initial positions (not at collision) and momenta at time  $t = 0$ , a unique solution exists on a maximal interval  $[0, t^*)$ . If  $t^* < \infty$  then the solution is said to have a singularity at  $t^*$ . The only singularities which occur in the collinear three-body problem are due to collision [12], though non-collision singularities have been found for other  $N$ -body problems [16].

Double collisions can be regularized. That is, one can change variables so that double collision transforms to a regular point of the flow [3]. This extension corresponds to an elastic bounce. McGehee further showed that triple collision is not regularizable. However, in McGehee coordinates, the flow is bounded by an invariant compact manifold which correspond to triple collision. The flow on this invariant manifold, called the collision manifold, guides solutions which pass near triple collision.

We change from Hamiltonian to McGehee coordinates via three steps. First is a change of variables to polar coordinates. Second is a time scaling change of variable so that solutions slow down as they pass near triple collision. Finally, one regularizes binary collisions.

The remainder of this section is a review of the change of variables to McGehee coordinates. Readers familiar with this material should feel free to pass on to the next section.

Let  $\mathbf{q} = (q_1, q_2, q_3) \in \mathbb{R}^3$  be the vector of positions. Define  $p_i = m_i \dot{q}_i$  and let  $\mathbf{p} = (p_1, p_2, p_3) \in \mathbb{R}^3$  be the vector of momenta. Let

$$M = \begin{pmatrix} m_1 & 0 & 0 \\ 0 & m_2 & 0 \\ 0 & 0 & m_3 \end{pmatrix}.$$

Then Equations 1 and 2 can be rewritten as

$$U(\mathbf{q}) = \sum_{i>j} \frac{m_i m_j}{q_i - q_j}$$

$$(3) \quad M \ddot{\mathbf{q}} = -\nabla U(\mathbf{q}).$$

We can also write the kinetic energy for the system as

$$T(\mathbf{p}) = \frac{1}{2} \mathbf{p}^T M \mathbf{p}.$$

The Hamiltonian for the system is

$$H(\mathbf{q}, \mathbf{p}) = T(\mathbf{p}) - U(\mathbf{q}),$$

and Equation 3 can be written as the system

$$(4) \quad \begin{aligned} \dot{\mathbf{q}} &= H_{\mathbf{p}}(\mathbf{q}, \mathbf{p}) = M^{-1} \mathbf{p} \\ \dot{\mathbf{p}} &= -H_{\mathbf{q}}(\mathbf{q}, \mathbf{p}) = -\nabla U(\mathbf{q}). \end{aligned}$$

The function  $T$  is defined everywhere in  $\mathbb{R}^3$ . The function  $U$  is defined everywhere except at collisions.

Next we break up  $\mathbf{q}$  into radial and angular components. Define

$$r = (\mathbf{q}^T M \mathbf{q})^{1/2}.$$

Notice that a level set of  $r$  is an ellipsoid in  $\mathbb{R}^3$ . Let  $S = \{\mathbf{q} \mid r = 1\}$ . Then a point in  $S$  is called a configuration for the system of particles.

We now define the variables:

$$\begin{aligned} r &= (\mathbf{q}^T M \mathbf{q})^{1/2} \\ \mathbf{s} &= r^{-1} \mathbf{q} \\ y &= \mathbf{p}^T \mathbf{s} \\ \mathbf{x} &= \mathbf{p} - y M \mathbf{s}. \end{aligned}$$

In these coordinates,  $r$  is the size of the configuration in a inertial norm,  $\mathbf{s} \in S$  is the configuration and represents the direction of  $\mathbf{q}$ ,  $y$  is the projection of  $\mathbf{p}$  in the direction of  $\mathbf{q}$  and  $\mathbf{x}$  represents the direction of change in the configuration. Note that  $\mathbf{s}$  and  $\mathbf{x}$  are orthogonal.

In the new polar coordinates, the Hamiltonian,  $H(\mathbf{q}, \mathbf{p}) = h$  can be written as

$$\frac{1}{2}(\mathbf{x}^T M^{-1} \mathbf{x} + y^2) - r^{-1} U(\mathbf{s}) = h$$

and the equations of motion become

$$\begin{aligned} \dot{r} &= y \\ \dot{y} &= r^{-1} \mathbf{x}^T M^{-1} \mathbf{x} - r^{-2} U(\mathbf{s}) \\ \dot{\mathbf{s}} &= r^{-1} M^{-1} \mathbf{x} \\ \dot{\mathbf{x}} &= -r^{-1} y \mathbf{x} - r^{-1} (\mathbf{x}^T M^{-1} \mathbf{x}) + r^{-2} U(\mathbf{s}) M \mathbf{s} + r^{-2} \nabla U(\mathbf{s}). \end{aligned}$$

We next introduce two new coordinates,  $\mathbf{u} = r^{1/2} \mathbf{x}$  and  $v = r^{1/2} y$  and scale time via  $dt = r^{3/2} dt'$ . In these time-scaled coordinates, the Hamiltonian,  $H(\mathbf{q}, \mathbf{p}) = h$  can be written as

$$\frac{1}{2}(\mathbf{u}^T M^{-1} \mathbf{u} + v^2) - U(\mathbf{s}) = rh$$

and the equations of motion become

$$\begin{aligned} \dot{r} &= rv \\ \dot{v} &= \frac{1}{2} v^2 + \mathbf{u}^T M^{-1} \mathbf{u} - U(\mathbf{s}) y \\ \dot{\mathbf{s}} &= M^{-1} \mathbf{u} \\ \dot{\mathbf{u}} &= -\frac{1}{2} v \mathbf{u} - (\mathbf{u}^T M^{-1} \mathbf{u}) M \mathbf{s} + U(\mathbf{s}) M \mathbf{s} + \nabla U(\mathbf{s}). \end{aligned}$$

We reduce the dimension of System 4 by fixing the center of mass at the origin and setting the total momentum to zero. This reduces the problem to a four-dimensional phase space.

To express this reduced system, note that there is a unique point on  $S$  so that  $q_1 = q_2 < q_3$  and the center of mass,  $M\mathbf{q} = 0$ . Call this unique point  $\mathbf{a} = (a_2, a_2, a_3)$ . Likewise, there is a unique point on  $S$  so that  $q_1 < q_2 = q_3$  and the center of mass,  $M\mathbf{q} = 0$ . Call this unique point  $\mathbf{b} = (b_1, b_2, b_2)$ . One can compute that  $0 < \mathbf{a}^T M \mathbf{b} < 1$ . Let  $\lambda$  be the least positive solution to

$$\cos(2\lambda) = \mathbf{a}^T M \mathbf{b}.$$

We now introduce an angular potential function,

$$W(s) = \frac{2}{\lambda} (W_1(s) + W_2(s) + W_3(s)) \sin(2\lambda)$$

where

$$\begin{aligned} W_1(s) &= \frac{m_1 m_2 (1-s)}{(b_2 - b_1) \operatorname{Sn}(\lambda(1+s))} \\ W_2(s) &= \frac{m_2 m_3 (1+s)}{(a_3 - a_2) \operatorname{Sn}(\lambda(1-s))} \\ W_3(s) &= \frac{\lambda m_1 m_3 (1-s^2)}{(b_2 - b_1) \sin(\lambda(1+s)) + (a_3 - a_2) \sin(\lambda(1-s))} \end{aligned}$$

and

$$\operatorname{Sn}(x) = \frac{\sin(x)}{x}.$$

To regularize double collisions, we introduce a new variable,

$$w = \frac{(1-s^2)u}{\sqrt{W(s)}}.$$

and scale time again via,

$$dt' = \frac{\lambda(1-s^2)}{\sqrt{W(s)}} d\tau.$$

Finally, we are ready to write System 4 in McGehee coordinates.

$$\begin{aligned} \frac{dr}{d\tau} &= \frac{\lambda(1-s^2)}{\sqrt{W(s)}} rv \\ \frac{dv}{d\tau} &= \frac{\lambda}{2} \sqrt{W(s)} \left( 1 - \frac{(1-s^2)}{W(s)} (v^2 - 4rh) \right) \\ \frac{ds}{d\tau} &= w \\ (5) \quad \frac{dw}{d\tau} &= -s + \frac{2s(1-s^2)}{W(s)} (v^2 - 2rh) + \frac{W'(s)}{2W(s)} (1-s^2-w^2) - \frac{\lambda(1-s^2)}{2\sqrt{W(s)}} vw. \end{aligned}$$

In McGehee coordinate, the Hamiltonian,  $H(\mathbf{q}, \mathbf{p}) = h$  can be rewritten as

$$(6) \quad W(s)(w^2 + s^2 - 1) + (1-s^2)^2(v^2 - 2rh) = 0$$

System 5 is defined for all values of  $r, v, s$  and  $w$ . Note that  $s$  is the configuration coordinate and varies from  $-1$  to  $1$ . The configuration  $s = -1$  corresponds to  $q_1 = q_2 < q_3$ , a left binary collision. The configuration  $s = 1$  corresponds to  $q_1 < q_2 = q_3$ , a right binary collision. Moreover, the vector fields is now defined at  $r = 0$ , triple collision.

When  $r = 0$  the Hamiltonian  $H = h$  in Equation 6 yields the relation

$$(7) \quad W(s)(w^2 + s^2 - 1) + (1-s^2)^2(v^2) = 0.$$

Equation 7 defines a manifold,  $\mathbf{M}$ , in  $\mathbb{R}^3$ , called the *collision manifold*, which is independent of the total energy,  $h$ . The phase space for System 5 is bounded by  $\mathbf{M}$ .

### 3. MCGEHEE COORDINATES

We briefly describe the flow in McGehee coordinates, summarizing results from McGehee's research [9]. For the rest of the paper, we assume that the total energy,  $h$ , is negative.

The function,  $W(s)/(1-s^2)$  has exactly one critical point at  $s_c$ . Let

$$v_c = \sqrt{\frac{W(s_c)}{1-s_c^2}}.$$

System 5 has two equilibria, both of which lay on the collision manifold,  $\mathbf{M}$ . The  $(r, v, s, w)$ -coordinates of these two equilibria are  $c = (0, -v_c, s_c, 0)$  and  $d = (0, v_c, s_c, 0)$  (see Figure 1)

On the collision manifold,  $c$  and  $d$  each have a one-dimensional stable manifold and a one-dimensional unstable manifold. The flow on the collision manifold is gradient-like with respect to level sets of  $v$  (that is,  $dv/d\tau \geq 0$  on  $\mathbf{M}$ ). A sketch of these stable and unstable manifolds is given in Figure 2.

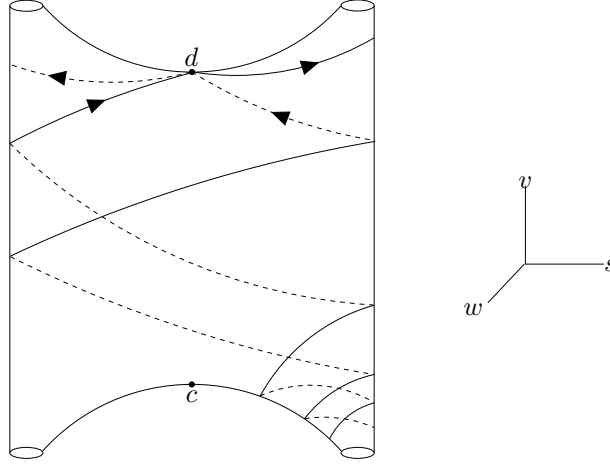


FIGURE 1. Collision manifold with stable and unstable branches of  $d$  on  $\mathbf{M}$ .

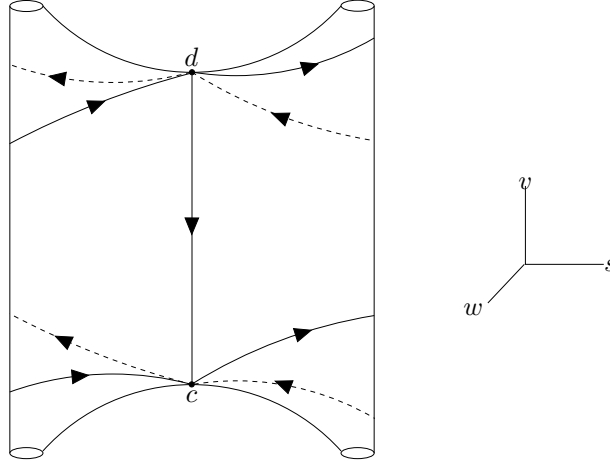


FIGURE 2. Ejection-collision orbit with stable and unstable branches of  $c$  and  $d$  on  $\mathbf{M}$ .

There is a heteroclinic connection between  $c$  and  $d$  corresponding to an ejection-collision orbit (see Figure 2). This solution is homographic, that is, the configuration is constant. So, along the ejection-collision orbit, the  $s$ -coordinate is constant,  $s_c$ . The forward solution of the orbit limits onto  $c$  and the backwards limit is  $d$ . Thus the ejection-collision orbit begins and ends at triple collision and does not pass through a binary collision.

We say any solution which has a forward limit on  $c$ , “ends in triple collision” and we say any solution which has a backwards limit from  $d$ , “begins in ejection”. The set of solutions which end in triple collision forms the two-dimensional stable manifold of  $c$ ,  $W^s(c)$  and the set of solutions which begin in ejection forms the two-dimensional unstable manifold of  $d$ ,  $W^u(d)$ . Any orbit in the intersection of  $W^s(c)$  and  $W^u(d)$  is called an ejection-collision solution.

Binary collisions occur at  $s = \pm 1$ . The energy relation in Equation 7 requires  $w = 0$  at binary collision. Thus we must use both the  $r$  and  $v$  coordinates distinguish one binary collision from another. Although the System 5 appears to separate the  $r$ -coordinate from the others (and indeed does so for  $|s| < 1$ ), we will have to include the  $r$ -coordinate at binary collisions.

All solutions, except for the homographic ejection-collision orbit, pass through at least one binary collision. This makes the pair of half planes,

$$\Gamma = \{(r, v, s, w) \mid r \geq 0, |s| = 1, w = 0\}$$

the appropriate choice for a Poincaré slice. Thanks to work by Mayer and Wang, we know something about the geometry of the intersection of the stable manifold for triple collision and this Poincaré slice,  $\Gamma$ .

The motivation for studying how the stable manifold intersect the Poincaré slice is given by the following argument. Any point on the Poincaré slice has a forward itinerary of binary collisions, perhaps ending in triple collision. Given a continuous arc on the Poincaré slice whose endpoints have different itineraries, there must be some point on the arc which is also on  $W^s(c)$ . That is,  $W^s(c)$  divides the Poincaré slice into regions with different itineraries.

We distinguish the two half-planes of the Poincaré slice by  $L$  for  $s = -1$ , and  $R$  for  $s = 1$ . The intersections of  $W^s(c)$  with  $L$  and  $R$  are arcs with two endpoints on  $r = 0$  or loops with one endpoint on  $r = 0$ . We label these arcs and loops by their itineraries using  $L$ 's and  $R$ 's for binary collisions and  $C$  for triple collision. We use the subscript  $*$  to designate the location of the set with a given itinerary. For example the itinerary  $LL_*RC$  is the set of initial conditions on  $L$  which in forward time pass through  $R$  once before triple collision and in backwards time pass through  $L$  again. The itinerary  $LLR_*C$ , however, designates the set of initial conditions on  $R$  which lead directly to triple collision and whose prior two binary collisions were on  $L$ .

Solutions on  $\mathbf{M}$ , may lay on the stable manifold for  $c$  or for  $d$ . Such solutions will terminate with the symbol  $c$  or  $d$  as appropriate. For example,  $L_*Rc$  designates the initial condition on  $\mathbf{M}$  which traverses to  $R$  and then limits onto  $c$  without passing through another binary collision. Likewise,  $L_*Ld$  designates the point on  $\mathbf{M}$  which begins on  $L$ , returns to  $L$  and then limits onto  $d$  without passing through another binary collision. Using this itinerary notation for the intersections of  $W^s(c)$  and the Poincaré slice, we next summarize Meyer and Wang's results [11] in the setting of McGehee coordinates.

There is a unique arc on  $L$  with itinerary  $L_*C$  (see Lemma 4.1). This arc has two endpoints on  $\mathbf{M}$ , one with the itinerary  $L_*c$  and the other  $L_*d$ . Likewise, there is a unique arc on  $R$  with itinerary  $R_*C$ . Its endpoints have itineraries  $R_*c$  and  $R_*d$  (see Figure 3). We know these arcs are unique since they must each be homotopic to the ejection-collision orbit between  $c$  and  $d$  which passes through no binary collisions.

To designate a solution which begins in ejection we use the symbol  $E$ . For example,  $ELR_*LC$  designates the initial condition(s) on  $R$  which pass through  $L$  and limit onto  $c$ . These initial condition(s) must also in backwards time pass through  $L$  then limit onto  $d$  without passing through any other binary collisions.

Intersections of the ejection manifold,  $W^u(d)$ , with the Poincaré slice have a simple relation to intersections of  $W^s(c)$  because System 5 is reversible. That is, it

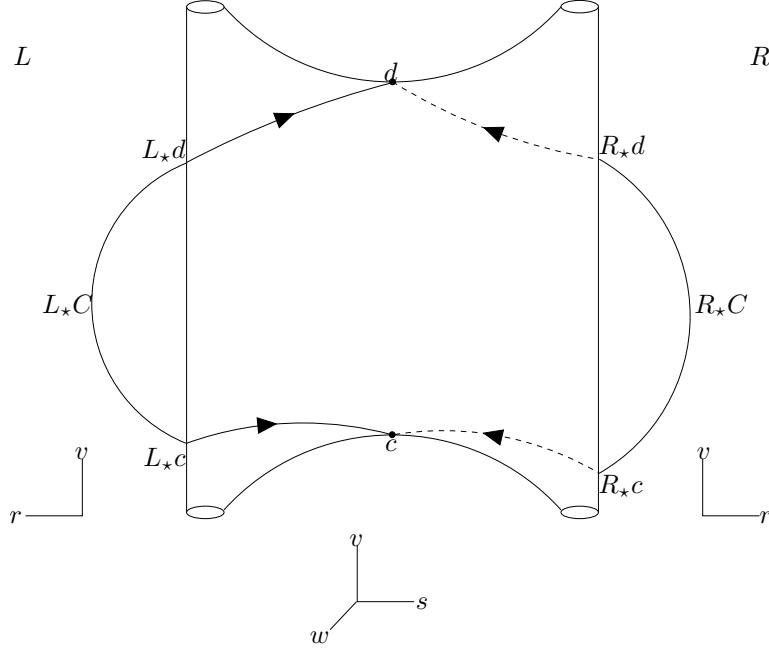


FIGURE 3. First pullback of stable manifold for triple collision.

has a time symmetry. Let

$$\begin{aligned}\bar{v} &= -v \\ \bar{w} &= -w \\ \bar{\tau} &= -\tau.\end{aligned}$$

If  $(r, v, s, w)$  is a solution in time  $\tau$ , then so is  $(r, \bar{v}, s, \bar{w})$  in time  $\bar{\tau}$ .

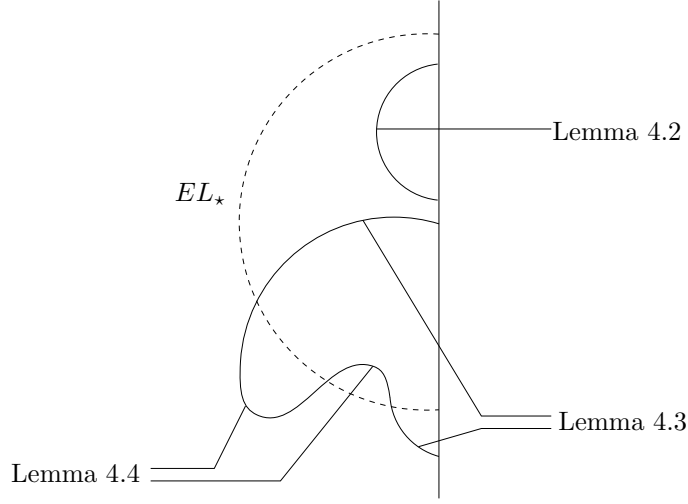
This means that the arcs  $L_*C$  and  $EL_*$  are reflections of one another over the  $v = 0$  axis. In general the arc or loop with itinerary  $a_0.a_1a_2\dots a_kC$  flips about the  $v = 0$  axis to an arc or loop with the itinerary  $Ea_k\dots a_2a_1a_0$ . and vice versa.

With the itinerary notation, we can briefly describe the work of Meyer and Wang. They generate their main results by focusing on regions whose itinerary begins  $L_*L$ ,  $L_*RL$ ,  $L_*RRL$ , and in general  $L_*R^nL$  (where  $R^n$  denotes a string of  $n$   $R$ 's). These regions are bounded by pieces of stable manifold whose itinerary is  $LR^nC$ . They show that the first return of these regions to  $L$  generates a sub-shift on an infinite number of symbols. Since not all regions are guaranteed to intersect the first returns, the exact dynamics can not be established although it is clear that the dynamics are rich.

#### 4. THE STABLE MANIFOLD OF TRIPLE COLLISION

In this section we characterize pullbacks of the stable manifold for triple collision,  $W^s(c)$ , on  $L$  and  $R$ . Recall we are studying the dynamics of the System 5. We have chosen a Poincaré slice,  $\Gamma$ , which is transverse to the flow [9] made up of two half-planes,  $L$  and  $R$ , corresponding to left and right binary collisions. The flow induces a map on  $\Gamma$ . We denote this Poincaré (first return) map by  $P$ . We now want to show how the stable manifold for triple collision,  $W^s(c)$ , intersects  $\Gamma$ .



FIGURE 4. Typical arcs on  $L$  labeled with corresponding Lemmas.

**Lemma 4.1.** *The first pull backs of the collision manifold,  $L_\star C$  and  $R_\star C$ , are smooth arcs with end points  $L_\star c$ ,  $L_\star d$  and  $R_\star c$ ,  $R_\star d$ .*

*Proof.* Since the flow is smooth,  $L_\star C$  and  $R_\star C$  are deformations of the ejection-collision orbit between  $c$  and  $d$ . Hence  $L_\star C$  and  $R_\star C$  are smooth arcs with end points on  $\mathbf{M}$ . Since the endpoints must limit to  $c$  and  $d$ , the endpoints of  $L_\star C$  are  $L_\star c$  and  $L_\star d$ . Likewise, the endpoints of  $R_\star C$  are  $R_\star c$  and  $R_\star d$ .  $\square$

We now show how to continue pulling back pieces of stable manifold for triple collision (see Figure 4). The following Lemmas are consistent with Meyer and Wang's results. However, Meyer and Wang proved them for the case where left binary collisions were not regularized. Here, we show them for the fully regularized system.

**Lemma 4.2.** *If an arc,  $\gamma$  in  $W^s(c) \cap \Gamma$  has endpoints  $x$  and  $y$  on  $\mathbf{M}$  and the arc does not intersect  $EL_\star$  or  $ER_\star$  then the pullback of  $\gamma$ , is an arc on  $\Gamma$  with endpoints  $P^{-1}(x)$  and  $P^{-1}(y)$  on  $\mathbf{M}$ .*

*Proof.* Clearly,  $x$  pulls back to  $P^{-1}(x)$ . Points on  $\gamma$  near  $x$  pull back near  $P^{-1}(x)$ . The only obstruction to pulling back a point on  $\gamma$  to  $\Gamma$  is if the point pulls back to ejection. Since  $\gamma$  has no such obstruction, all of  $\gamma$  pulls back to  $\Gamma$  as described.  $\square$

**Lemma 4.3.** *If an arc in  $W^s(c) \cap \Gamma$  has endpoints  $x$  and  $y$  on  $\mathbf{M}$  and the arc intersects  $EL_\star$  or  $ER_\star$  then the segment,  $\delta$ , from  $x$  (or  $y$ ) to the first intersection with  $EL_\star$  or  $ER_\star$  pulls back to an arc on  $\Gamma$  with endpoints  $P^{-1}(x)$  (or  $P^{-1}(y)$ ) and either  $L_\star d$  if the segment pulls back to  $L$  or  $R_\star d$  if the segment pulls back to  $R$ .*

*Proof.* Assume that  $\delta$  has an endpoint at  $x$ . Clearly,  $x$  pulls back to  $P^{-1}(x)$ . Points on  $\delta$  near  $x$  pull back near  $P^{-1}(x)$ . We continue pulling back points along  $\delta$ . Points near the intersection of  $\delta$  and  $EL_\star$  or  $ER_\star$  must pull back arbitrarily close

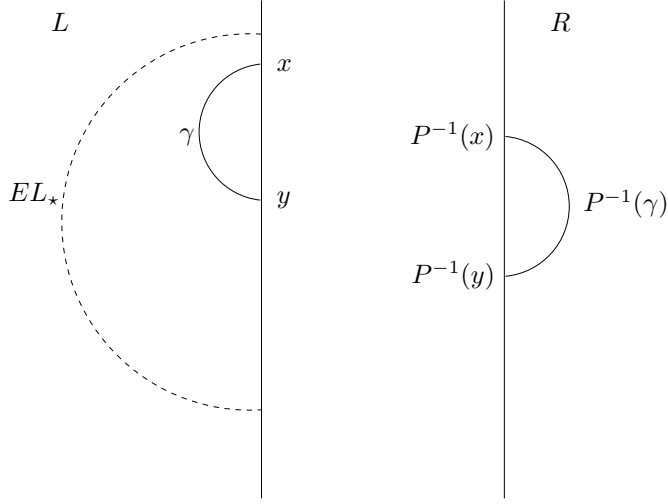


FIGURE 5. An arc and its pullback for Lemma 4.2.

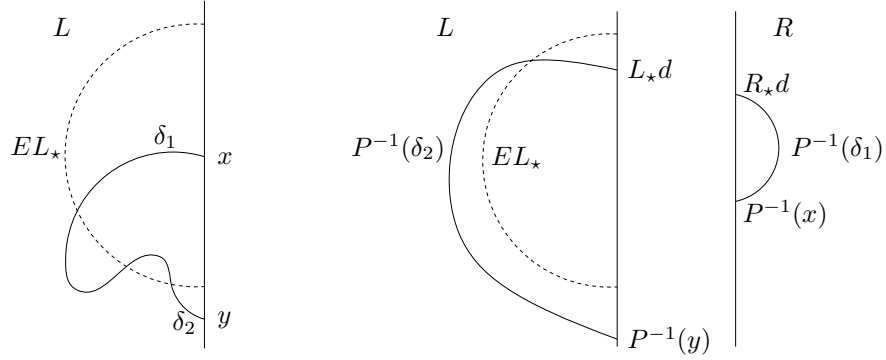


FIGURE 6. Two arc segments and their pullbacks for Lemma 4.3.

to the equilibrium,  $d$ , hence return to  $\Gamma$  arbitrarily close to one branch of the stable manifold for  $d$  on  $\mathbf{M}$ . Thus points on  $\delta$  near the intersection of  $\delta$  and  $EL_*$  or  $ER_*$  must pull back to  $\Gamma$  arbitrarily close to either  $L_*d$  or  $R_*d$ . By continuity, points near the intersection of  $\delta$  and  $EL_*$  or  $ER_*$  must pull back to the same half-plane,  $L$  or  $R$ , as the rest of  $\delta$ .

□

**Lemma 4.4.** *If a segment of an arc,  $\delta$ , in  $W^s(c) \cap \Gamma$  has both endpoints on  $EL_*$  or  $ER_*$  and has no other intersections with  $EL_*$  or  $ER_*$ , then the segment pulls back to a loop on  $\Gamma$  with both endpoints at either  $L_*d$  if the segment pulls back to  $L$  or  $R_*d$  if the segment pulls back to  $R$ .*

*Proof.* Since  $\delta$  intersects  $EL_*$  or  $ER_*$  only at its endpoints, all of  $\delta$  pulls back to either  $L$  or  $R$ . Points on  $\delta$  near the intersections of  $\delta$  and  $EL_*$  or  $ER_*$  must pull back arbitrarily close to the equilibrium,  $d$ , hence return to  $\Gamma$  arbitrarily close to one branch of the stable manifold for  $d$  on  $\mathbf{M}$ . Thus points on  $\delta$  near the intersections

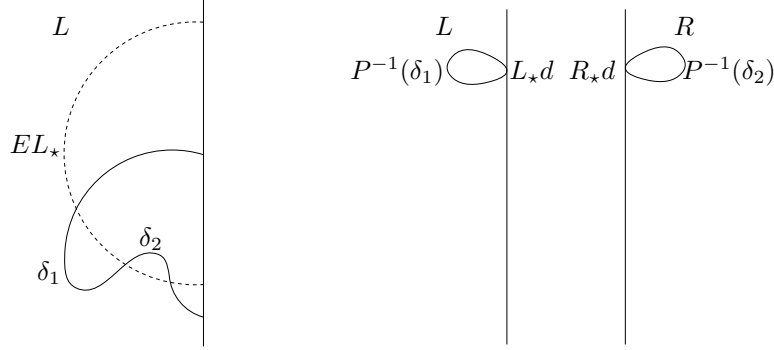


FIGURE 7. Two arc segments and their pullbacks for Lemma 4.4.

of  $\delta$  and  $EL_*$  or  $ER_*$  must pull back to  $\Gamma$  arbitrarily close to either  $L_*d$  if the rest of  $\delta$  pulls back to  $L$  or  $R_*d$  if the rest of  $\delta$  pulls back to  $R$ .

Pullbacks of loops are covered in earlier Lemmas since we may let  $x = y$  in Lemma 4.2.  $\square$

By the lemmas above, we know that the endpoints of arcs and loops in  $W^s(c) \cap \Gamma$  are on either the stable manifold of  $c$  or  $d$  on  $\mathbf{M}$ . By McGehee, we know that the stable manifold for  $c$  has two branches on  $\mathbf{M}$ . The stable manifold for  $d$  has two branches. In backwards time, one branch passes first through  $L$  and then alternates between  $R$  and  $L$ , eventually going down one of the legs. The other branch of  $W^s(d)$  on  $\mathbf{M}$  in backwards time passes first through  $R$  and then alternates between  $L$  and  $R$ , eventually going down one of the legs (see Figure 1).

One branch of  $W^s(d)$  on  $\mathbf{M}$  has an itinerary  $\dots LLLRLRL\dots Ld$ . We denote the length of the alternating part of this itinerary  $\ell_{\mathbf{M}}$ . Likewise, we denote the length of the alternating part of the branch of  $W^s(d)$  ending  $\dots Rd$  by  $r_{\mathbf{M}}$ . For example, a branch of  $W^s(d)$  on  $\mathbf{M}$  with itinerary  $\dots LLLRLRLd$  yields  $\ell_{\mathbf{M}} = 5$ .

Since the branches of  $W^s(d)$  can not intersect we have the relation

$$(8) \quad |\ell_{\mathbf{M}} - r_{\mathbf{M}}| \leq 1.$$

If  $\ell_{\mathbf{M}} = r_{\mathbf{M}}$  then either each branch goes down a different leg of  $\mathbf{M}$  or there is a heteroclinic connections between  $c$  and  $d$  on  $\mathbf{M}$ , i.e.  $W^s(d) = W^u(c)$ . Otherwise  $\ell_{\mathbf{M}}$  and  $r_{\mathbf{M}}$  differ by one and both branches must go down the same leg.

McGehee shows that the  $v$ -coordinate along flow on  $\mathbf{M}$  is non-decreasing. Meyer and Wang show that the stable branches for  $d$  on  $\mathbf{M}$  must end with  $RLd$  or  $LRd$ . That is,

$$\ell_{\mathbf{M}}, r_{\mathbf{M}} \geq 2.$$

These two facts have the following geometric consequence.

**Lemma 4.5.** *The stable manifold of  $c$  with itinerary  $L_*C$  and the unstable manifold with itinerary  $EL_*$  intersect on  $L$ . Likewise,  $R_*C$  and  $ER_*$  intersect on  $R$ .*

*Proof.* We only look at the case of the intersection of  $L_*C$  and  $EL_*$  on  $L$  since the other case is similar.

Let  $v(x)$  be the  $v$ -coordinate of a point on  $\mathbf{M}$ . Since  $v$  is non-decreasing along solutions on  $\mathbf{M}$ , we know from the definition of stable and unstable manifolds that

the following inequality holds

$$v(L_*C) \leq v(c) < 0 < v(d) \leq v(dL_*)$$

If  $v(L_*d) \leq v(cL_*)$ , then the inverse image of  $L_*d$  under the Poincaré map must be on  $L$  since the pullback of  $L_*d$  can not intersect the trajectory between  $c$  and  $cL_*$ . This means that one branch of the stable manifold for  $d$  on  $\mathbf{M}$  would have the itinerary  $LLd$  which contradicts Meyer and Wang's result. Thus  $v(cL_*) \leq v(L_*d)$ . Since  $v(cL_*) + v(L_*d) = 0$  we have the inequality

$$(9) \quad v(L_*C) \leq v(c) \leq v(cL_*) \leq 0 \leq v(L_*d) \leq v(d) \leq v(dL_*)$$

The continuous arc  $L_*C$  has endpoints at  $L_*c$  and  $L_*d$ . The continuous arc  $EL_*$  has endpoints at  $dL_*$  and  $cL_*$ . By the inequality in Equation 9,  $L_*C$  and  $EL_*$  must intersect at least once.  $\square$

The segment of  $L_*C$  from  $L_*d$  to the first intersection of  $EL_*$  by Lemma 4.3 must pullback under  $P^{-1}$  to an arc on  $R$  with endpoints at  $R_*Ld$  and  $R_*d$ . If this arc does not intersect  $ER_*$  then we continue pulling back this segment until there is a first intersection with either  $EL_*$  or  $ER_*$ . Denote by  $\ell_\cap$  the number of pullbacks required for the first intersection. Likewise, let  $r_\cap$  denote the number of pullbacks required for the segment of  $R_*C$  from  $R_*d$  to the first intersection with  $ER_*$  to next intersect  $EL_*$  or  $ER_*$ .

## 5. MAIN RESULTS

The Lemmas of the previous section establish that  $W^s(c) \cap \Gamma$  is made up smooth arcs and loops whose endpoints are on the stable manifolds of  $c$  and  $d$  on  $\mathbf{M}$ . Thus  $W^s(c) \cap \Gamma$  generates an infinite number of regions on  $\Gamma$ . However, only a finite number of regions are needed to determine or bound the symbolic dynamics.

The values of  $\ell_{\mathbf{M}}$ ,  $r_{\mathbf{M}}$ ,  $\ell_\cap$ , and  $r_\cap$  characterize the global dynamics. The following theorems connect  $\ell_{\mathbf{M}}$ ,  $r_{\mathbf{M}}$ ,  $\ell_\cap$ , and  $r_\cap$  with the global dynamics.

Before proceeding, we review the definition of a sofic system. A finite directed graph whose arrows are labeled and the labels may be used more than once is called a *sofic* system. The dual to a sofic system, then, is a finite directed graph whose vertices are labeled and whose labels may be used more than once. Sofic systems are a generalization of sub-shifts of finite type. See [15] and [8] for more information on sofic systems and their role in dynamical systems.

**Theorem 5.1.** *If for three given masses  $\ell_{\mathbf{M}} = r_{\mathbf{M}} = \ell_\cap + 1 = r_\cap + 1$  then the set of allowed itineraries for the system is given by the dual of a sofic system (see Figures 10 and 11).*

*Proof.* The arc  $EL_*$  divides  $L$  into two regions. We call the bounded region the *inside* of  $EL_*$  and the unbounded region the *outside* of  $EL_*$ . Likewise, we define the inside of  $ER_*$  and the outside of  $ER_*$ .

We next divide the inside of  $EL_*$  into a finite number of regions via the following procedure. The segment(s) of  $L_*C$  inside  $EL_*$  is (are) the primary left segment(s), denoted  $PLS$ . Note that the segment of  $L_*C$  from  $L_*d$  to the first intersection with  $EL_*$  is always contained in the  $PLS$ . If  $PLS$  contains any other segments, they must be of the form described by Lemma 4.4.

By the definition of  $\ell_\cap$ , the first  $\ell_\cap - 1$  pullbacks of  $PLS$  are (or at least contain) arcs inside  $ER_*$  and  $EL_*$ . We call these arcs  $PLS^{-1}$ ,  $PLS^{-2}$ , ...,  $PLS^{-\ell_\cap+1}$  successively. Likewise, we define  $PRS$  and its pullbacks,  $PRS^{-1}$ ,  $PRS^{-2}$ , ...,  $PRS^{-\ell_\cap+1}$ .

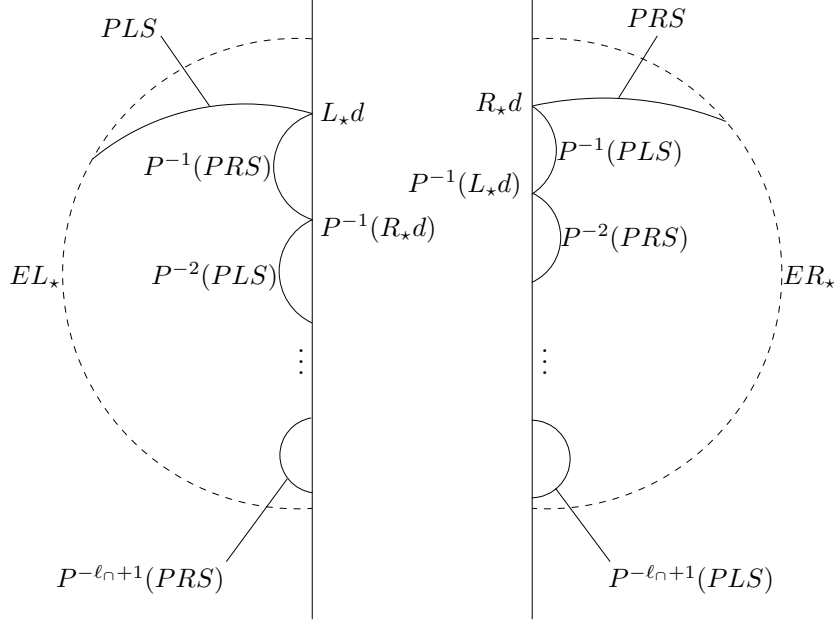


FIGURE 8. Dividing  $L$  and  $R$  each into  $\ell_\cap + 2$  regions. Diagram labeled for  $\ell_\cap$  even.

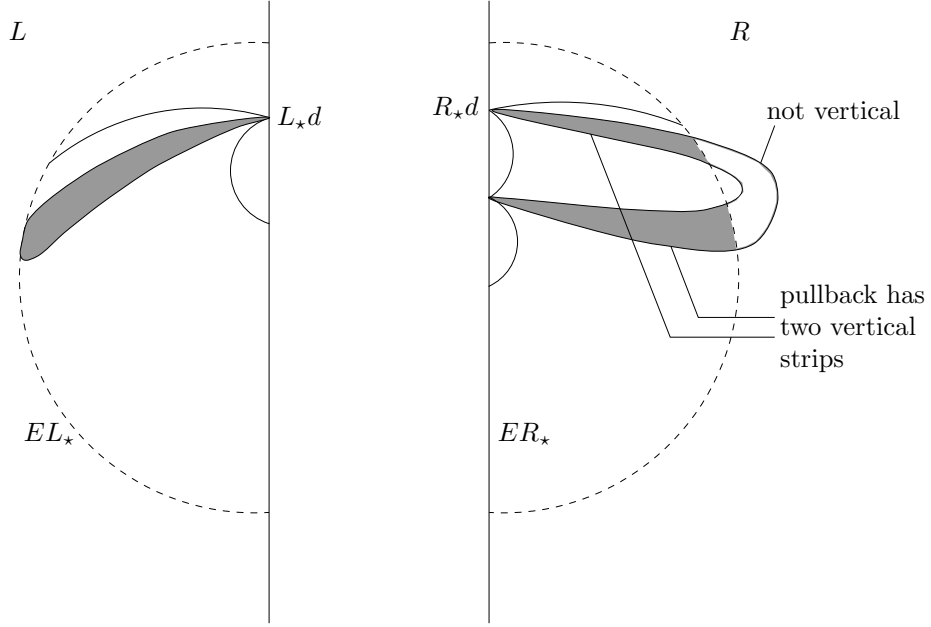
The arcs,  $EL_*$ ,  $ER_*$ ,  $PLS$  and its pullbacks and  $PRS$  and its pullbacks divide  $L$  and  $R$  each into  $\ell_\cap + 2$  regions. Figure 8 describes the case where  $PLS$  and  $PRS$  each only have one segment. If they had additional segments, loops would be attached at the pullbacks of  $L_*d$  and/or  $R_*d$ .

Points on  $\mathbf{M}$  of the form  $P^{-2i}(L_*d)$  or  $P^{-2i+1}(R_*d)$  ( $i \geq 0$ ) which are in the closure of the inside of  $EL_*$  are called *inside points* of  $EL_*$ . Likewise, points on  $\mathbf{M}$  of the form  $P^{-2i}(R_*d)$  or  $P^{-2i+1}(L_*d)$  ( $i \geq 0$ ) which are in the closure of the inside of  $ER_*$  are called *inside points* of  $ER_*$ . Points on  $\mathbf{M}$  of the form  $P^{-i}(R_*d)$  or  $P^{-i}(L_*d)$  which are not inside points are called *outside points*.

We define a *vertical strip* as a simply connected subset of a region whose intersection with the boundary of the region is made up of one of the following:

1. at least one inside point and a segment of  $EL_*$  or  $ER_*$
2. at least one outside point and a segment of  $EL_*$  or  $ER_*$
3. at least two inside points
4. at least two outside points

The pullback of an inside point is either an inside point or an outside point. The pullback of an outside point is an outside point. The pullback of a region arbitrarily near  $EL_*$  or  $ER_*$  is a region either arbitrarily near  $L_*d$  or  $R_*d$ . So the pull back of a vertical strip at least contains vertical strips. If the pullback of a vertical strip crosses over  $EL_*$  or  $ER_*$ , two segments of the pullback are vertical strips while the rest of the segments only have ends on  $EL_*$  or  $ER_*$ , and hence are not vertical (see Figure 9).

FIGURE 9. Shaded vertical strip on  $L$  and its pullback on  $R$ .

Although we can make a directed graph showing how regions map to one another under  $P^{-1}$ , we must also show that the pull back of a region's vertical strip contain vertical strips in the pullback of the region.

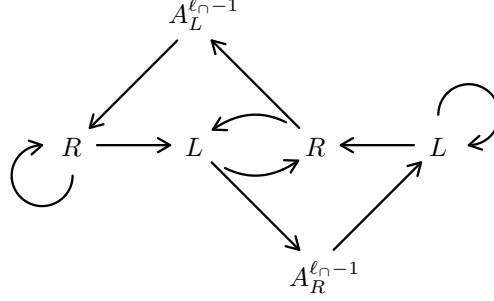
We next describe the pullbacks of various cases of vertical strips. Our goal is to show that the division of  $L$  and  $R$  described above is a Markov partition of  $\Gamma$  for  $P^{-1}$  (hence Markov for  $P$  by reversability).

We begin with a vertical strip inside  $EL_*$  and above the arc of  $PLS$  from  $L_*d$  to the first intersection with  $EL_*$ . This vertical strip pulls back to a vertical strip between  $R_*d$  and  $RL_*d$  inside  $PLS^{-1}$ . Further pulls backs generate vertical strips in regions bounded  $PLS^{-i}$  for  $1 \leq i \leq \ell_\cap - 1$ .

A vertical strip inside  $PLS^{\ell_\cap+1}$  contains at least two vertical strips. One strip includes a segment of  $EL_*$  or  $ER_*$  and the outside point,  $P^{-\ell_\cap}(L_*d)$ . The other strip includes  $EL$  and the inside point  $P^{-\ell_\cap+1}(R_*d)$ . This second strip, though inside  $EL_*$  or  $ER_*$  is also outside the regions  $PLS^{-i}$  or  $PRS^{-i}$  for  $1 \leq i \leq \ell_\cap - 1$ .

A vertical strip from  $EL_*$  or  $ER_*$  to any outside point has a pullback which includes a vertical strip from inside  $EL_*$  or  $ER_*$  and above either the arc of  $PLS$  from  $L_*d$  to the first intersection with  $EL_*$  or the arc of  $PRS$  from  $R_*d$  to the first intersection with  $ER_*$ .

Like a vertical strip inside  $PLS^{\ell_\cap+1}$ , a vertical strip from a segment of  $EL_*$  or  $ER_*$  and with  $P^{-\ell_\cap+1}(L_*d$  or  $P^{-\ell_\cap+1}(R_*d)$  contains at least two vertical strips. One strip includes a segment of  $EL_*$  or  $ER_*$  and the outside point,  $P^{-\ell_\cap}(L_*d)$ . The other strip includes  $EL$  and the inside point  $P^{-\ell_\cap+1}(R_*d)$ . This second strip, though inside  $EL_*$  or  $ER_*$  is also outside the regions  $PLS^{-i}$  or  $PRS^{-i}$  for  $1 \leq i \leq \ell_\cap - 1$ .

FIGURE 10. Directed graph for Theorem 5.1 where  $\ell_n$  is even.

The above argument can be repeated beginning with a vertical strip inside  $ER_\star$  and above the arc of  $PRS$  from  $R_\star d$  to the first intersection with  $ER_\star$ .

Since vertical strips in a region pull back to vertical strips in the pullback of the region, the partition of  $L$  and  $R$  given above is Markov. If we label the regions, then there is a subshift of finite type which semi-conjugate to  $P^{-1}$  on  $\Gamma$ . By reversability, we can switch the direction of the arrows and get a subshift of finite type which is semi-conjugate to  $P$  on  $\Gamma$ .

Replacing region names with “ $L$ ” for regions on  $L$  and “ $R$ ” for regions on  $R$  yields a directed graph on two symbols (the dual of a sofic system). This directed graph in general can be simplified. The simplified graph describes all itineraries of binary collisions.

To see this last claim, any initial condition on  $L$  or  $R$  is in some region as defined above. Thus the point maps about the regions according to some path in the sub-shift, so its itinerary is described by the graph.

Conversely, given any itinerary described by the graph, there is at least one path in the sub-shift which accomplishes the given itinerary. Choose a closed vertical strip in the first region for such a path. Since the pullback of vertical strips includes contains vertical strips we can generate a nested sequence of closed vertical strips which obtain arbitrarily many terms in the desired sequence. The infinite intersection of these closed and nested vertical strips is non-empty, thus guaranteeing at least one point which achieves the given itinerary.  $\square$

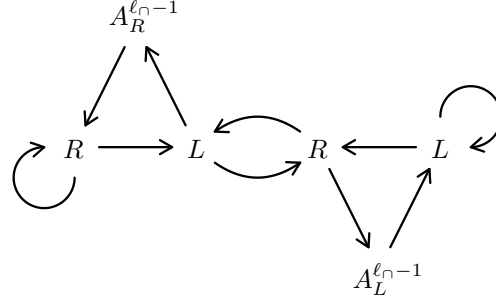
Carrying out the procedure outlined in Theorem 5.1 we see that for the case  $\ell_M = r_M = \ell_n + 1 = r_n + 1$ , the generated dual to a sofic system is given by Figures 10 and 11. Note that the symbol  $A_L^{\ell_n-1}$  means an alternating sequence of  $L$ ’s and  $R$ ’s beginning with  $L$  of length  $\ell_n - 1$ . Likewise, the symbol  $A_R^{\ell_n-1}$  means an alternating sequence of  $L$ ’s and  $R$ ’s beginning with  $R$  of length  $\ell_n - 1$ .

Note that for  $\ell_M = r_M = \ell_n + 1 = r_n + 1 = 2$  the dual to a sofic system reduces to the full shift on two symbols.

**Theorem 5.2.** *If for three given masses  $\ell_M = r_M + 1 = r_n + 2 \leq \ell_n$  or  $r_M = \ell_M + 1 = \ell_n + 2 \leq r_n$  then the set of itineraries for the system is bounded between two duals of sofic systems (see Figures 12 to 15).*

*Proof.* We will assume the first case,  $\ell_M = r_M + 1 = r_n + 2 \leq \ell_n$ , since the argument for the second case is similar.

Using the notation from Theorem 5.1 we divide the inside of  $EL_\star$  and  $ER_\star$  into a finite number of regions bounded by  $PLS^{-i}$  for  $0 \leq i \leq r_n$  and  $PRS^{-i}$  for

FIGURE 11. Directed graph for Theorem 5.1 where  $\ell_\cap$  is odd.

$0 \leq i \leq r_\cap - 1$ . We also make regions outside  $ER_\star$  or  $EL_\star$  bounded by  $PLS^{-i}$  for  $r_\cap + 1 \leq i \leq \ell_\cap - 1$ .

By the argument in Theorem 5.1, a region's vertical strip pulls back to vertical strips in the region's pullbacks with one exception. A vertical strip inside  $PLS^{-\ell_\cap+1}$  will not pull back to a vertical strip inside  $EL_\star$  or  $ER_\star$  even though the region bounded by  $PLS^{-\ell_\cap+1}$  and  $\mathbf{M}$  must cross either  $EL_\star$  or  $ER_\star$ . This means that a directed graph showing how regions map under  $P^{-1}$  will not be Markov. However a point on  $\Gamma$  must move from region to region according to the the directed graph so the directed graph contains all allowed itineraries of regions even though some itineraries may not be achieved.

So we begin with the directed graph showing how regions map under  $P^{-1}$ . By reversability, switching the direction of the arrows we have a directed graph showing how regions map under  $P$ . Replacing region names with “ $L$ ” for regions on  $L$  and “ $R$ ” for regions on  $R$  yields a directed graph on two symbols (the dual of a sofic system). This directed graph in general can be simplified. The simplified graph contains all itineraries of binary collisions.

To bound the set of allowed itineraries from below, we assume that pullbacks of  $PLS$  never intersect  $EL_\star$  or  $ER_\star$ . That is we assume  $r_\cap = +\infty$ . Although this is not the case, the condition guarantees a region's vertical strips pull back to vertical strips in the pullback of the region. That is, the directed graph showing how regions map under  $P^{-1}$  with the condition that  $r_\cap = +\infty$  is Markov, hence the sub-shift contains orbits which are guaranteed to occur in the actual system.

We begin with the directed graph showing regions map under  $P^{-1}$  with the condition that  $r_\cap = +\infty$ . By reversability, switching the direction of the arrows we have a directed graph showing how regions map under  $P$ . Replacing region names with “ $L$ ” for regions on  $L$  and “ $R$ ” for regions on  $R$  yields a directed graph on two symbols (the dual of a sofic system). This directed graph in general can be simplified. The simplified graph contains all guaranteed itineraries of binary collisions.  $\square$

Carrying out the procedure outlined in Theorem 5.2 we see that for the case  $\ell_\mathbf{M} = r_\mathbf{M} + 1 = r_\cap + 2 \leq \ell_\cap$ , the generated duals to sofic systems is given by Figures 12 to 15. For the case  $r_\mathbf{M} = \ell_\mathbf{M} + 1 = \ell_\cap + 2 \leq r_\cap$ , the generated duals to sofic systems is given by Figures 12 to 15 after exchanging  $L$ 's and  $R$ 's.

**Theorem 5.3.** *If for three given masses, if  $\ell_\mathbf{M}, r_\mathbf{M}, \ell_\cap$  and  $r_\cap$  do not meet the criteria of Theorem 5.1 or Theorem 5.2 then the set of itineraries for the system is bounded between two duals of sofic systems.*



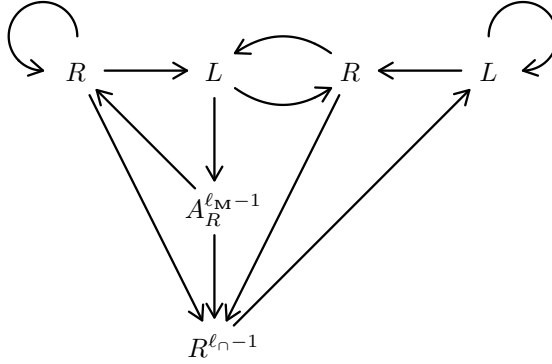


FIGURE 12. Directed graph for Theorem 5.2 containing allowed sequences for  $\ell_M$  even.

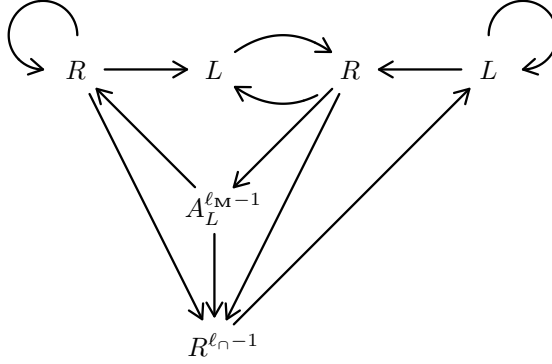


FIGURE 13. Directed graph for Theorem 5.2 containing allowed sequences for  $\ell_M$  odd.

*Proof.* If  $\ell_M, r_M, \ell_\cap$  and  $r_\cap$  do not meet the criteria of Theorem 5.1 or Theorem 5.2 then (using the notation of Theorem 5.1) one of the pull backs of  $PLS$  or  $PRS$  must cross  $EL_\star$  or  $ER_\star$  when both of endpoints of that arc are either inside  $EL_\star$  or  $ER_\star$ . This means that a vertical strip which landed in this region will pass to a non-vertical strip outside  $EL_\star$  or  $ER_\star$ , even though the region pulls back outside  $EL_\star$  or  $ER_\star$ . This means a Markov partition is not possible for a directed graph on any finite set of regions similar to Theorem 5.1 or Theorem 5.2.

If  $\ell_M = r_M$  then the directed graph from Theorem 5.1 for these values of  $\ell_M$  and  $r_M$  must contain guaranteed dynamics for our system since the premature intersection described above only adds to the possible set of itineraries.

Likewise, if  $\ell_M \neq r_M$  then the associated directed graph from Theorem 5.2 which contains guaranteed sequences also contains guaranteed sequences for our system since the premature intersection described above only adds to the possible set of itineraries.

To get an upper bound for our system we divide  $L$  and  $R$  into a finite number of regions bounded by  $EL_\star$ ,  $ER_\star$ ,  $PLS^{-i}$  for  $0 \leq i \leq \ell_\cap - 1$  and  $PRS^{-i}$  for  $0 \leq i \leq r_\cap - 1$ . Each of these pullbacks are single arcs by the conditions on  $\ell_\cap$  and  $r_\cap$ . The directed graph describing how these regions map under  $P^{-1}$  must contain all allowed itineraries of regions even though some itineraries may not be achieved.

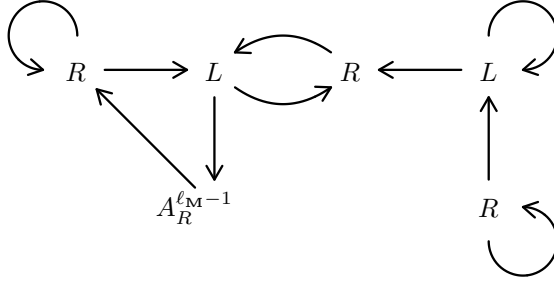


FIGURE 14. Directed graph for Theorem 5.2 containing guaranteed sequences for  $\ell_{\mathbf{M}}$  even.

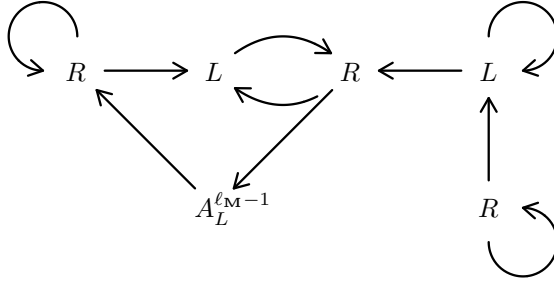


FIGURE 15. Directed graph for Theorem 5.2 containing guaranteed sequences for  $\ell_{\mathbf{M}}$  odd.

So we begin with the directed graph showing how regions map under  $P^{-1}$ . By reversability, switching the direction of the arrows we have a directed graph showing how regions map under  $P$ . Replacing region names with “ $L$ ” for regions on  $L$  and “ $R$ ” for regions on  $R$  yields a directed graph on two symbols (the dual of a sofic system). This directed graph in general can be simplified. The simplified graph contains all itineraries of binary collisions.  $\square$

Carrying out the procedure outlined in Theorem 5.3 as an example, we see that for the case  $\ell_{\mathbf{M}} = 5, r_{\mathbf{M}} = 6, \ell_{\cap} = 2$  and  $r_{\cap} = 7$ , the generated dual to a sofic system containing all allowed sequences is given by Figure 16.

Note that for  $\ell_{\cap} = r_{\cap} = 1$  the upper bound for the dynamics is the full shift on two symbols, hence a trivial upper bound.

## 6. OSCILLATORY MOTION

One application of the Theorems in Section 5 is to the presence of oscillatory motion in the  $N$ -body problem. Saari and Xia explored possible behaviors in the  $N$ -body problem as  $t \rightarrow \infty$  [14]. One such behavior is oscillatory motion, that is, a mutual distance coordinate  $r$ , so that as  $t \rightarrow \infty$ , the  $\limsup r = \infty$  while the  $\liminf r < \infty$ .

For the collinear three-body problem, oscillatory motion requires that either  $m_1$  or  $m_3$  takes longer and longer excursions for the other binary pair, each time returning to the binary pair before its next excursion. Saari and Xia showed that

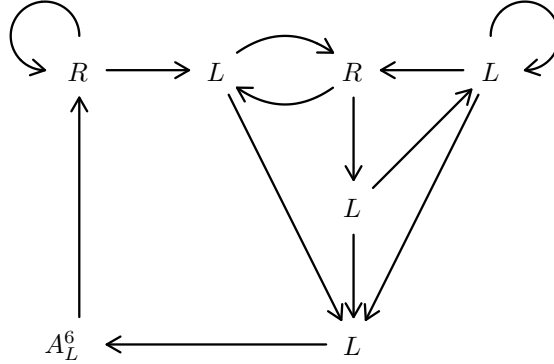


FIGURE 16. Directed graph for Theorem 5.3 containing all allowed sequences for the case  $\ell_{\mathbf{M}} = 5, r_{\mathbf{M}} = 6, \ell_{\cap} = 2$  and  $r_{\cap} = 7$ .

it is enough to prove the presence of itineraries of the form

$$\dots L^{a_1} \dots L^{a_2} \dots L^{a_3} \dots L^{a_4} \dots \quad \text{or} \quad \dots R^{a_1} \dots R^{a_2} \dots R^{a_3} \dots R^{a_4} \dots$$

so that  $a_i \rightarrow \infty$  as  $i \rightarrow \infty$ . The existence of such itineraries guarantees the existence of oscillatory motion.

Saari and Xia study the return map on the zero momentum set for  $m_3$ . To guarantee a return map, they restrict the masses to the case where triple collision can lead to arbitrarily high velocities. This is exactly when the stable manifold of  $d$  and the unstable manifold of  $c$  intersect transversely. In this case, the set of allowed itineraries is given by the full-shift on two symbols (same as  $\ell_{\mathbf{M}} = r_{\mathbf{M}} = \ell_{\cap} + 1 = r_{\cap} + 1 = 2$ ).

Once they establish the existence of oscillatory motion in the collinear three-body problem for some sets of masses, they note that the motion can be extended to the  $N$ -body problem. They conclude that for any  $N \geq 3$  there exist masses and initial conditions so that oscillatory motion exists.

From the Theorems in Section 5 it is clear that for all sets of masses which admit transverse intersections of the stable manifold of  $d$  and the unstable manifold of  $c$ , itineraries of the form

$$\dots L^{a_1} \dots L^{a_2} \dots L^{a_3} \dots L^{a_4} \dots \quad \text{or} \quad \dots R^{a_1} \dots R^{a_2} \dots R^{a_3} \dots R^{a_4} \dots$$

so that  $a_i \rightarrow \infty$  as  $i \rightarrow \infty$  exist. We are thus led to the same conclusion as a Corollary to our Theorems.

**Corollary 6.1.** *For the  $N$ -body problem,  $N \geq 3$ , there exist positive masses and initial conditions so that oscillatory motion occurs.*

#### REFERENCES

- [1] Benet, L., Trautmann, D., and Seligman, T.H., “Chaotic Scattering in the Restricted Three-Body Problem: I. The Copenhagen Problem”, *Celestial Mech. Dynam. Astronomy* **66** 203–228, 1997.
- [2] Chesley, S. and Zare, K., “Bifurcations in the Mass Ratio of the Planar Isosceles Three-Body Problem”, unpublished.
- [3] Easton, Robert, “The Topology of the Regularized Integral Surfaces of the 3-Body Problem”, *J. Diff. Eq.* **12** 361–384, 1972.

- [4] Kaplan, Samuel R., “The Collinear One-Bumper Two-Body Problem”, *Hamiltonian dynamics and celestial mechanics* (Seattle, WA, 1995), 87–107, *Contemp. Math.*, **198**, Amer. Math. Soc., Providence, RI, 1996.
- [5] Kaplan, Samuel R., “Dynamics of the Collinear One-Bumper Two-Body Problem”, *J. Diff. Eq.*, **140** no. 2, 378–414, 1997.
- [6] Kaplan, Samuel R., “The Collinear One-Bumper Two-Body Problem with Unequal Masses”, *Dynamics and Stability of Systems*, **13** 27–54, 1998.
- [7] Kaplan, Samuel R., “The Collision Manifold of the Collinear One-Bumper Two-Body Problem”, submitted to *Celestial Mech. Dynam. Astronomy*, March, 1998.
- [8] Lind, Douglas and Marcus, Brian, *An Introduction to Symbolic Dynamics and Coding*, Cambridge University Press, Cambridge, England, 1995.
- [9] McGehee, Richard, “Triple Collision in the Collinear Three-Body Problem”, *Inventiones mathematicae* **27**, 191–227, 1974.
- [10] Meyer, K. R. and Hall, G. R., “Introduction to Hamiltonian Dynamical Systems and the  $N$ -Body Problem”, Springer-Verlag, Berlin, 1992.
- [11] Meyer, K. R. and Wang, Q. D., “The Collinear Three-Body Problem with Negative Energy”, *J. Diff. Eq.* **119**, no. 2, 284–309, 1995.
- [12] Painlevé, P., *Lecons sur la théorie analytique des equations différentielles*, Sotckholm, 1895.
- [13] Poincaré, Henri, “Sur les problèmes des trois corp et les equations dynamique”, *Acta Mathematica* **13**, 1–270, 1890.
- [14] Saari, Donald G. and Xia, Zhihong, “The existence of oscillatory and superhyperbolic motion in Newtonian systems”, *J. Diff. Eq.* **82**, no. 2, 342–355, 1989.
- [15] Weiss, B., “Subshifts of Finite Type and Sofic Systems”, *Montats. Math.* **77** 462–474, 1973.
- [16] Xia, Zhihong, “The existence of noncollision singularities in Newtonian systems”, *Ann. of Math.*, **135** no. 3, 411–468, 1992.

DEPARTMENT OF MATHEMATICS, BOWDOIN COLLEGE<sup>1</sup> BRUNSWICK, ME 04011

---

<sup>1</sup>The author is presently at the University of North Carolina at Asheville, Asheville, NC 28801